APPLICATION OF A DOMAIN DECOMPOSITION TECHNIQUE TO THE MATHEMATICAL MODELLING OF A SOLID FUEL COMBUSTION CHAMBER OF A RAMJET

P. J. Coelho*, N. Duic** and, M.G. Carvalho*

* Instituto Superior Técnico, Technical University of Lisbon
Mechanical Engineering Department
Av. Rovisco Pais, 1096 Lisboa Codex, Portugal

** Faculty of Mechanical Engineering and Naval Architecture
University of Zagreb, Salajeva 5, 41000 Zagreb, Croatia

ABSTRACT

A computer code aimed at the simulation of the physical phenomena occurring in the solid fuel combustion chamber of a ramjet was extended to accommodate multi-block grids. The mathematical model is based on the numerical solution of the governing equations for mass, momentum, energy and transport equations for scalar quantities. The k-ε model and the conserved scalar/prescribed probability density function formalism are employed. Heat and mass transfer at the walls are calculated using the wall functions of Chieng and Launder modified to account for porous walls. The multi-block method allows discontinuous grid lines along the interblock boundaries and transfer of data between neighboring blocks satisfies flux conservation. The model was applied to a ramjet combustor, and the influence of the air mass flow rate, inlet air temperature, and pressure were investigated. The multi-block predictions corroborate previous single-bock results, indicating a marked increase of the regression rate with the increase of inlet air temperature and air mass flow rate, and a marginal increase with pressure, for the range considered in the analysis. The characteristic velocity increases with the rise of pressure, but decreases with the air mass flow rate.

NOMENCLATURE

a_N	—	Combined convection/diffusion coefficient
c^*	—	Characteristic velocity
C_p	—	Specific heat at constant pressure
C_μ	—	Constant of the turbulence model
E	—	Constant in near-wall description of the velocity profile
f	—	Weighting factor
F	—	Flux
h_v	—	Effective heat of gasification
k	—	Turbulent kinetic energy
M	—	Molar mass of the mixture
P	—	Jayatillaka function
q_w	—	Heat flux to the wall
r	—	Regression rate; radial coordinate
R	—	Radius
R_0	—	Universal gas constant
T	—	Temperature
u	—	Velocity component parallel to the wall
U	—	Mean inlet velocity
v_w	—	Velocity of the fuel blown through the wall
y	—	Distance to the wall
γ	—	Ratio of specific heats
Γ	—	Vandenkerckhove function
κ	—	Von Karman constant
μ	—	Dinamic viscosity
ν	—	Kinematic viscosity
ρ	—	Density
σ_t	—	Constant of the turbulence model
ϕ	—	Arbitrary scalar variable
τ	—	Shear stress

Subscripts

f_u	—	Fuel
P	—	Grid node close to the wall
v	—	Viscous sublayer/fully turbulent region interface
w	—	Wall

INTRODUCTION

Nowadays, ramjets are drawing attention throughout the world because of their potential military and civilian applications. They can be used for the propulsion of missiles and projectiles, and for hypersonic or orbital aircrafts and space launchers. Compared to conventional rocket propulsion systems, ramjet propelled vehicles offer a considerable performance gain, because they use the oxygen in the atmosphere for combustion, instead of carrying the oxidizer. They have the potential to achieve an increased range and they offer increased effectiveness against maneuvering targets. The solid fuel ramjet is especially attractive for the propulsion of projectiles, because it is simple, cheap and has a high fuel density.

Figure 1 shows a sketch of a solid fuel ramjet combustor. It consists of an inlet, a solid fuel combustion chamber, and a nozzle. The incoming air is decelerated by shockwaves in the inlet to low subsonic velocities, yielding an increase of pressure and temperature. At the

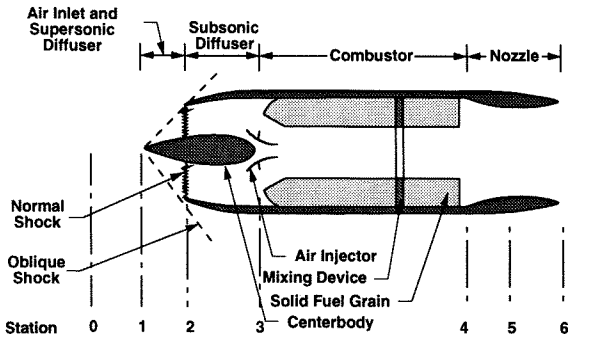

STATION NUMBER	LOCATION
0	Vehicle flow field immediately uperstream of the air induction system
1	Capture sation-beginnging of internal flow system
2	Cowl lip
3	Diffuser exit-combustor entrance
4	Combustor exit
5	Nozzle throad
6	Nozzle exit

Figure 1 - Schematic of a ramjet combustor

combustion chamber inlet, a diaphragm creates a sudden expansion of the incoming air, originating a recirculation zone required for flame stabilization. The recirculation zone contributes to increase the residence time of the gases in the combustor and it enhances the mixing of fuel and oxidizer. The solid fuel grain is a hollow cylinder which is pyrolyzed by the hot air. A gas phase diffusion flame resultant from the reaction between the fuel vapors and the air increases the temperature in the combustion chamber. In the nozzle, the thermal energy is converted to kinetic energy, yielding thrust.

The design of solid-fuel ramjet combustors has generally been based on empirical methods[1-2] and correlations[3-5], although more fundamental mathematical models have also been developed[6-7]. At the TNO Prins Maurits Laboratory, in the Netherlands, the flow and combustion processes in a solid fuel combustion chamber have been studied both theoretically and experimentally[8-13]. A computer code, COPPEF, was developed to simulate the physical phenomena taking place in the combustion chamber[8-9]. This code was recently extended in order to handle multi-block grids.[14]

The need for efficient flow solvers for engineering flow problems in complex geometries has motivated the development of several domain decomposition techniques, namely overlapping grids, multi-block grids and local grid refinement. Nowadays, these techniques are extensively used in aeronautics to compute flows around wings and aircrafts. However, they have received much less attention in the calculation of low Mach number flows using pressure correction solvers.

The objective of this paper is to apply the multi-block domain decomposition technique recently reported and validated[14] to the investigation of the performance of a ramjet combustor under several different operating conditions. Such a parametric study had already been carried out using single-block grids and the original COPPEF code.[13] Here, the aim is to perform a similar analysis using to multi-block capability recently incorporated in the code, consolidating the validation studies presented in Coelho et al.[14]

In the next section, the computational model describing the flow and combustion processes will be presented focusing on the calculation of the heat transfer and the solid fuel regression rate at the solid fuel wall. The multi-block domain decomposition technique is described next. Then, the results obtained are presented and discussed. Conclusions are drawn in the last section.

THE MATHEMATICAL MODEL

In the present work the COPPEF computer code developed by Vos[8-9] and recently extended to accommodate a multi-block grid[14] was used. This code is aimed at the calculation of turbulent flows in two-dimensional Cartesian or axisymmetric geometries, and it includes subroutines suitable for the simulation of a solid fuel combustion chamber of a ramjet. Before addressing the extension to multi-block grids, a brief overview of the physical models is given. Further details may be found elsewhere[8-9].

The mathematical model is based on the solution of the Favre-averaged conservation equations for mass, momentum, energy and transport equations for scalar quantities. The Reynolds stresses and the turbulent scalar fluxes are estimated using the k-ε eddy viscosity/diffusivity turbulence model. Combustion is modeled using the conserved scalar/prescribed probability density function (p.d.f.) formalism. It is assumed that combustion is described by a single one-step irreversible reaction between the fuel and the oxidizer yielding combustion products. This assumption provides relationships between instantaneous values of the chemical species concentrations and the conserved scalar, taken as the mixture fraction.

The mean values of the chemical species concentrations may be found from integration of the product of the instantaneous concentrations by the p.d.f. over the mixture fraction range. The beta p.d.f. was chosen. It is completely defined in terms of the mean value and variance of the mixture fraction. Transport equations are solved to compute these two quantities. A finite rate chemical kinetics combustion model is also available in the code. However, it does not account for the turbulence/combustion interaction and, therefore, it was not used in the present calculations.

The k-ε turbulence model is not valid close to the walls, where the Reynolds number is low. In such regions, the wall functions of Chieng and Launder[15], modified to account for porous walls with blowing or suction, were employed. These wall functions play a crucial role in the determination of the regression rate, a very important parameter in the analysis of solid fuel combustion chambers. The calculation of this rate is explained below.

The wall function method of Chieng and Launder assumes that the boundary layer near a solid wall can be divided into two regions, a viscous sublayer, in the immediate vicinity of the wall, and a fully turbulent region. The interface between the two regions is located

at $Re_V = 20$. Re_V is the Reynolds number based on the distance to the wall, y_V, and on the local square root of the turbulent kinetic energy, k_V. The turbulent kinetic energy is assumed to have a parabolic distribution in the viscous sublayer and a linear distribution in the fully turbulent region. This assumed distribution allows the calculation of y_V and k_V at the interface.

In the fully turbulent region, the velocity component parallel to the wall, estimated from a Couette flow analysis, is given by [16]:

$$u = \frac{\tau_w/\rho}{\kappa C_\mu^{1/4} k_v^{1/2}} \ln\left(E\, y\, C_\mu^{1/4} k_v^{1/2}/\nu\right) + v_w \left(\frac{\ln\left(E\, y\, C_\mu^{1/4} k_v^{1/2}/\nu\right)}{2\kappa}\right)^2 \quad (1)$$

where the second term accounts for blowing or suction effects. In this case, E is no longer a constant but depends on the local flow conditions. In the viscous sublayer the shear stress distribution is given by:

$$\tau = \tau_w + \rho\, v_w\, u = \mu \frac{du}{dy} \cong \mu \frac{u}{y} \quad (2)$$

Applying equation (1) to the grid node close to the wall, and applying equations (1) and (2) to the interface between the viscous sublayer and the fully turbulent region, a system of three equations is obtained from which τ_W, u_V and E may be calculated.

A Couette flow analysis also shows that the heat flux to the wall may be calculated as:

$$\frac{\rho C_P (T_w - T) k_v^{1/2} C_\mu^{1/4}}{q_w} = \left[\left(1 + \frac{v_w u_P}{\tau_w/\rho}\right)^{\sigma_t} \exp\left(\frac{\sigma_t v_w P}{k_v^{1/2} C_\mu^{1/4}}\right) - 1\right] / \left(v_w/\left(k_v^{1/2} C_\mu^{1/4}\right)\right) \quad (3)$$

The heat flux to the wall, q_W, may be related to the velocity of the fuel blown through the wall into the flow, v_W:

$$q_w = h_v\, \rho_{fu} v_w \quad (4)$$

where ρ_{fu} is the density of the gaseous fuel and h_V is the effective heat of gasification, i.e., the amount of heat required to pyrolyze 1 kg of fuel. Equations (3) and (4) are used to compute q_W and v_W. The local regression rate of the fuel, r, is then calculated from:

$$r = q_w/(\rho_w h_v) \quad (5)$$

where ρ_W is the density of the solid fuel.

The governing equations are integrated in each control volume using a finite-volume method and a multi-block domain decomposition technique, which is described in the next section. The equations are discretized using central differences for all but the convective terms which are discretized using the power-law scheme. A staggered grid variable arrangement is employed. Pressure-velocity coupling is accomplished by means of the SIMPLE, SIMPLEC or SIMPLER algorithms. A line continuity correction method is also incorporated. The solution of the systems of discretized equations is carried out using the Gauss-Seidel line-by-line iterative procedure.

THE MULTI-BLOCK DOMAIN DECOMPOSITION METHOD

In the multi-block method the physical domain is divided into several subdomains (blocks), and a grid is generated for each block separately. In this way, fine grids need only be used in regions of steep gradients, whereas coarse grids may be employed in regions of smooth variation of the dependent variables. To solve the governing equations in such a domain, information must periodically be exchanged among the blocks. This exchange of information is a key issue of a multi-block solver.

A staggered grid system is used in the COPPEF code. To allow for the exchange of information mentioned above, neighboring blocks overlap at the interblock boundaries in such a way that, for each block, one line of grid nodes is placed beyond the interblock boundary. An additional line is used to simplify the boundary conditions treatment. Figure 2 shows the grid structure at an interblock boundary.

In the multi-block method, each block is treated sequentially in each iteration. Solution of the governing equations in a given block requires the specification of the boundary conditions for that block. Part of the block boundary does not coincide with the boundary of the physical domain but it is shared with one or more other blocks. The identification of the kind of boundary for each grid node along the boundary, as well as the identification of the neighboring block in the case of an interblock boundary, is performed prior to the beginning of the iterative procedure and stored in an array.

One of the key features of the finite volume method is that it naturally ensures conservation of fluxes. Although conservation is easy to ensure if a single-block grid is considered, care must be taken when computing the fluxes across the interblock boundaries for multiblock grids, if conservation is to be maintained. To ensure conservation, the fluxes must be identical when estimated from the blocks on either side of an interblock boundary.

To explain the calculation of fluxes of scalar variables at the interblock boundaries, the example illustrated in Fig. 2 is considered. Let N be the block to be treated and NB the neighboring block. Suppose that IS and IE are the limits, in block N, of the interblock boundary between blocks N and NB. The south boundary of block NB is swept to identify the indices of the grid nodes of that block that share the interblock boundary with block N. Let ISNB and IENB be the lower and upper limits of the interblock boundary in block NB as shown in Fig. 2.

The governing equations are solved for block N up to J=JMAX-1 (see Fig. 2). Thus, a boundary condition involving data from block NB is required for

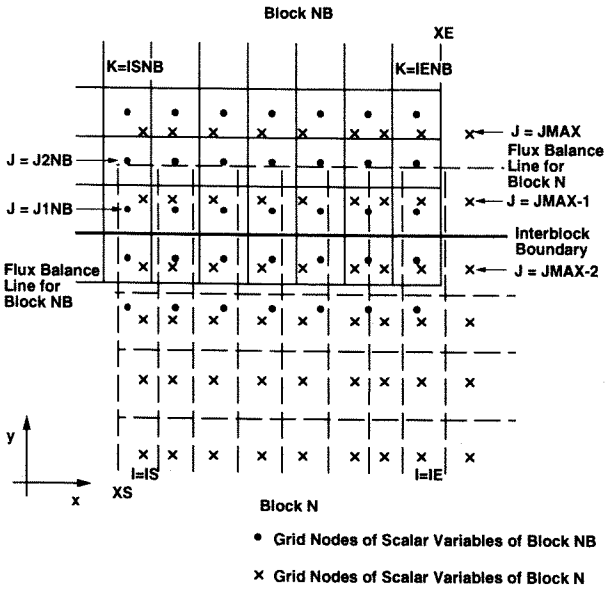

Figure 2 - Grid detail to illustrate the calculation of the fluxes

the north face of the control volumes of block N with J=JMAX-1. The line containing the north faces of such control volumes is referred to as the flux balance line for block N. A flux balance line for block NB may be defined similarly. The region between the two flux balance lines is the overlapping region.

Global flux conservation across the flux balance line requires that the following identity is satisfied

$$\int_{XS}^{XE} F^{(N)}(x)\,dx = \int_{XS}^{XE} F^{(NB)}(x)\,dx \qquad (6)$$

where XS and XE are the x limits of the interblock boundary between blocks N and NB, as shown in Fig. 2. $F^{(N)}$ and $F^{(NB)}$ are the fluxes computed for blocks N and NB, respectively.

Local flux conservation across the flux balance line requires that for every control volume of block N with index I such that IS ≤ I ≤ IE the following relation holds:

$$\int_{x_{i-1/2}^{(N)}}^{x_{i+1/2}^{(N)}} F^{(N)}(x)\,dx = \int_{x_{i-1/2}^{(N)}}^{x_{i+1/2}^{(N)}} F^{(NB)}(x)\,dx \qquad (7)$$

where $x_{i-1/2}^{(N)}$ and $x_{i+1/2}^{(N)}$ are the x coordinates of the cell faces of control volumes of block N with index I. Local flux conservation implies global flux conservation, i.e., satisfaction of equation (7) for all control volumes of block N such that IS ≤ I ≤ IE automatically ensures that equation (6) is also satisfied.

Discretization of equation (7) yields:

$$F_i^{(N)} = \sum_{k=ISNB}^{IENB} f_{i,k}\, F_k^{(NB)} \qquad (8)$$

where $f_{i,k}$ is a weighting factor equal to the fraction of the area of cell K (ISNB ≤ K ≤ IENB) of block NB that lies on the interblock boundary with cell I of block N.

The flux computation along the interblock boundary under consideration requires a sweep in block N from IS to IE and, for each I cell, involves the calculation of the flux $F_i^{(N)}$ according to equation (8). Other interblock boundaries are treated likewise.

The flux $F_k^{(NB)}$ of a scalar variable f across the flux balance line is calculated as follows:

$$F_k^{(NB)} = a_N \left(\phi_{k,\,J2NB}^{(NB)} - \phi_{k,\,J1NB}^{(NB)} \right) \qquad (9)$$

The combined convection/diffusion coefficient, a_N, is determined from the mass flow rate and the diffusion flux, both evaluated at the flux balance line using the data of block NB.

The treatment of the u-velocity component along horizontal interblock boundaries and of the v-velocity component along vertical interblock boundaries are similar to that described above. The differences resultant from grid staggering do not present any difficulties. The u velocity component, calculated from the convective flux at vertical flux balance lines, is used as a boundary condition for the u-momentum equation along vertical boundaries. Similarly, the v velocity component, calculated from the convective flux at horizontal flux balance lines, is used as a boundary condition for the v-momentum equation along horizontal boundaries.

The treatment described above does not apply to the pressure correction equation. In this case, the mass flow rate across an interblock boundary is calculated as in the other equations. The coefficient of the discretized equation for the cell face lying on the interblock boundary is set equal to zero and the mass flow rate is directly inserted into the source term.

In case of isothermal flows, the governing equations only involve pressure gradients. Hence, if a multi-block grid is employed, independent pressure fields may develop within each block, even if the pressure is prescribed at a certain location. In fact, due to the arrangement of staggered grid variables, the pressure within a block is not required to solve the equations in the neighboring blocks. Although this development of independent pressure fields does not prevent achieving convergence, it is not desirable whenever knowledge of the pressure field is important for the problem under consideration.

In case of reactive flows, the situation is more complex because the pressure field is used to compute the temperature by means of the equation of state. Therefore, if independent pressure fields were obtained in different blocks convergence could not be achieved. Hence, we have devised a simple method to adjust the pressure within the blocks, in such a way that the global pressure within the grid is identical to the one predicted using a single-block grid. The method consists of the selection of an interblock boundary for each block, calculation of the total pressure force along that interblock boundary for one of the blocks, and adjustment of the pressure field in

the other block, such that the total pressure force along the interblock boundary computed in each one of the two blocks is the same.

The multi-block strategy outlined above was incorporated in the COPPEF code. To improve convergence, global as well as block mass conservation was enforced during the course of the iterative procedure.

RESULTS AND DISCUSSION

The combustor chamber investigated here is schematically shown in Fig. 1. It has a length of 300 mm. The inner diameter of the combustion chamber increases along the time due to fuel (polyethylene) pyrolysis, but this process is not taken into account by the mathematical model. The initial fuel grain diameter is 40 mm but, since the experimental mean regression rate is about 0.2 mm/s, the fuel grain diameter was set equal to 45 mm for calculation purposes. This is an average value of the inner diameter during combustion for the measurements carried out. At standard operating conditions, air at a temperature of 300 K and a pressure of 0.45 MPa is admitted into the combustion chamber through a port of 15 mm diameter. The air mass flow rate is 150 g/s.

All the calculations were performed using the grid shown in Fig. 3. It has three blocks with discontinuous grid lines along the interblock boundaries.

During the first few iterations, large changes in the dependent variables occur from iteration to iteration, unless the initial guess is close to the converged solution. During iteration number n, when block number k is treated, n iterations have already been performed for blocks 1 to k-1, whereas only n-1 iterations have been performed for the remaining blocks. This causes large discontinuities in the pressure and velocity fields along the interblock boundaries at the beginning of the iterative procedure. These discontinuities induce high levels of turbulent kinetic energy and dissipation rate yielding divergence of the iterative procedure. To prevent the appearance of these unphysical high levels of k and ε, it is necessary to use small underrelaxation factors until a relatively stabilized velocity field has been established and unphysical gradients along the interblock boundaries have been eliminated. Hence, k and ε underrelaxation factors one order of magnitude smaller than their final values were used up to iteration number 30. Thereafter, they were multiplied by a factor 10 and kept unchanged up to the end of the convergence process.

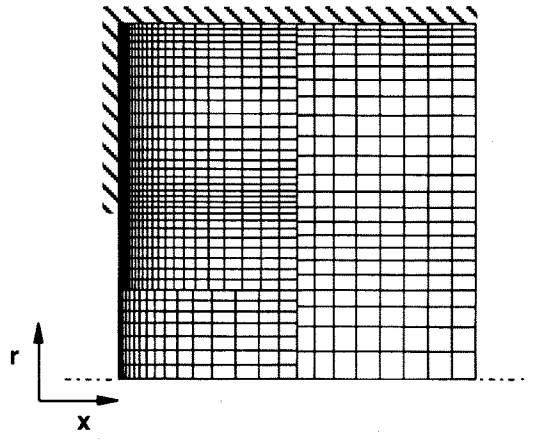

Figure 3 - Grid used to compute the flow in the solid fuel combustion chamber.

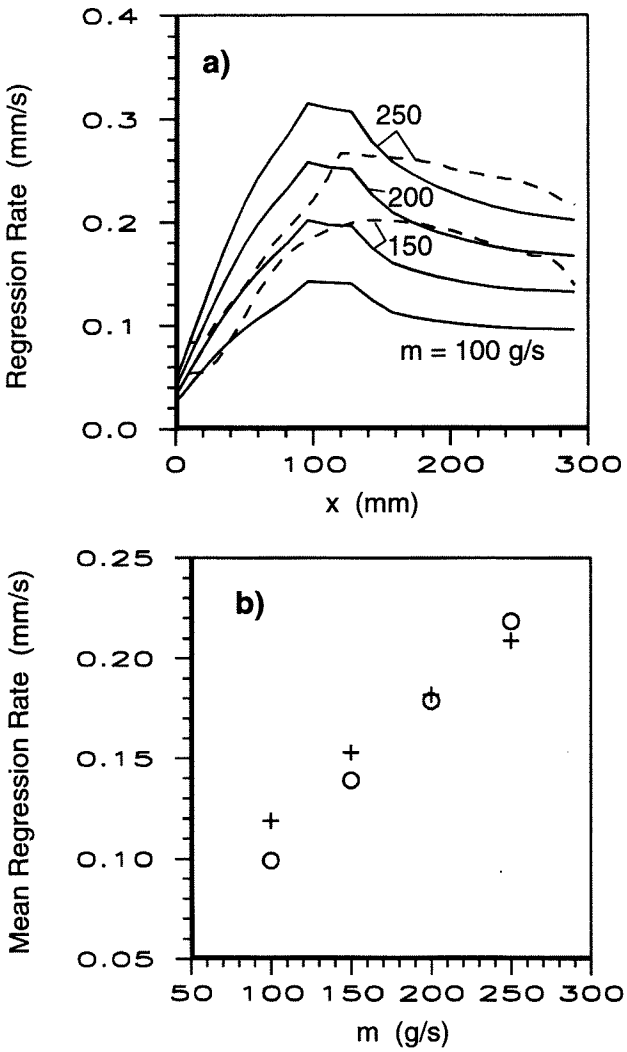

Figure 4 - Local and mean regression rate as a function of the air mass flow rate.
a) Solid line: predictions; dashed line: measurements
b) o: predictions; +: measurements

The predicted evolution of the local regression rate along the wall for air mass flow rates, m, in the range 100-250g/s is shown in Fig. 4a). Measurements[13] available for m=150 and 250g/s are also plotted. The predicted regression rate increases significantly along the streamwise direction up to the reattachment point, and decreases farther downstream approaching a constant value. If the air mass flow rate increases, the evolution remains qualitatively unchanged, but the regression rate increases. The measurements also exhibit a peak of the regression rate at the reattachment point which occurs farther downstream than in the predictions. This is consistent with the well known behaviour of the k-ε

model in this flow configuration[17]. Downstream of the reattachment point the measured regression rate decreases smoothly, while the predictions show a fast drop followed by a smooth decay farther downstream. Both the predicted and the measured mean regression rate increase with the air mass flow rate, but the predicted dependency is stronger than the experimental one, as shown in Fig. 4b).

The influence of the inlet air temperature on the local and mean regression rates is illustrated in Fig. 5. The dependency of the regression rate on the inlet air temperature is similar to the dependency on the air mass flow rate. Hence, the local regression rate along the wall increases, but its evolution remains qualitatively unchanged, when the inlet air temperature increases. The mean regression rate is underpredicted, as a result of the underestimation of the local regression rate downstream of the reattachment point.

Figure 6 shows the predicted local and mean regression rates as a function of the chamber pressure. At pressures below 0.5MPa the polyethylene yields very low soot concentration but, as the pressure increases, the soot concentration increases and so does the radiative heat transfer.[10] This heat transfer mechanism is not yet incorporated in the code and, therefore, the present study has only considered pressures up to 0.75 MPa. It has been experimentally observed[10] that there is hardly any pressure sensitivity on the regression rate for pressure chambers below 0.6MPa. These observations are consistent with the current calculations, which reveal a marginal increase of the local and mean regression rates with the pressure rise.

The predicted sensitivity of the local and mean regression rates on the air mass flow rate, inlet air temperature and chamber pressure follows the trends

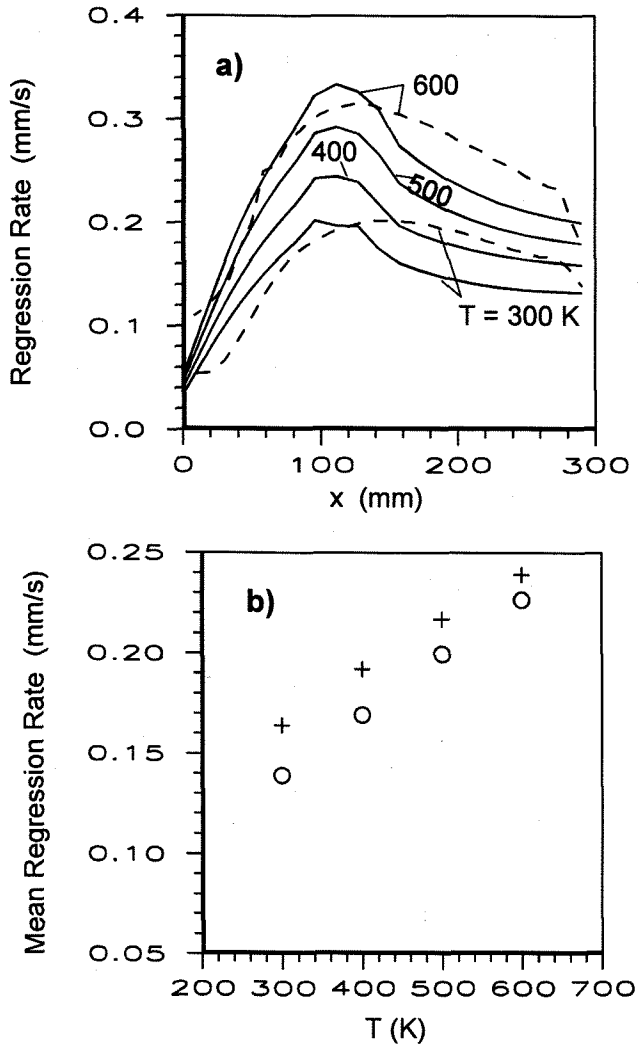

Figure 5 - Local and mean regression rate as a function of the inlet air temperature.
a) Solid line; predictions; dashed line: measurements.
b) o: predictions; + measurements

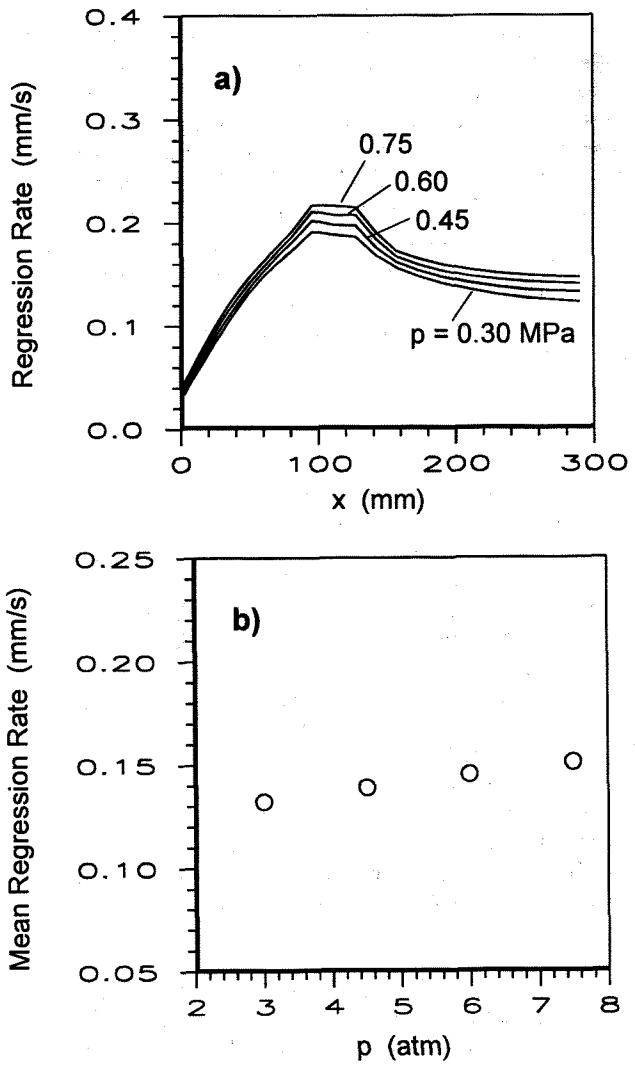

Figure 6 - Predicted local and mean regression rate as a function of the pressure.

previously reported for single-block grids.[13]

The performance of a solid fuel combustion chamber may be determined from the characteristic velocity. This velocity is defined as[18]:

$$C^*=(1/\Gamma)\sqrt{R_o T_c/M} \qquad (10)$$

where T_c is the local temperature and Γ is defined as:

$$\Gamma = \sqrt{\gamma}\,[2/(\gamma+1)]^{(\gamma+1)/2(\gamma-1)} \qquad (11)$$

The characteristic velocity may be used to determine the efficiency of the combustion process, defined as the ratio between the experimental and the theoretical characteristic velocities. The theoretical characteristic velocity as a function of the air mass flow rate and pressure chamber is plotted in Fig. 7. It was calculated by two different processes. In one of them the predicted average temperature at the exit section was used in equation (10). In the other one, chemical equilibrium was assumed and the corresponding temperature, calculated from a chemical equilibrium code[19], was used in equation (10).

Figure 7 shows that the characteristic velocity decreases with the increase of the air mass flow rate and increases with the increase of the chamber pressure, regardless of the method employed to calculate the temperature T_c. The calculation of the theoretical characteristic velocity using the equilibrium temperature yields lower values than using the predicted mean exit temperature. However, the differences are small and do not exceed 4% for the studied range of operating conditions.

CONCLUSIONS

A computer code aimed at the calculation of turbulent reactive flows in a solid fuel combustion chamber of a ramjet was recently extended to accommodate a multi-block domain decomposition technique. In case of multi-block calculations it is necessary to start the iterations with small values of the underrelaxation factors for the turbulent kinetic energy and dissipation rate equations, in order to prevent divergence of the iterative solution procedure. These factors may be increased after a relatively stable solution has been achieved.

The code was applied to the simulation of a ramjet combustor and several parametric studies were carried out, illustrating the influence of the air mass flow rate, inlet air temperature and pressure chamber on the regression rate and characteristic velocity. The multi-block predictions corroborate previous single-block results, indicating a marked increase of the regression rate with the increase of inlet air temperature and air mass flow rate, and a marginal increase with pressure, for the range considered in the analysis. The characteristic velocity increases with the rise of the pressure, but decreases with the air mass flow rate.

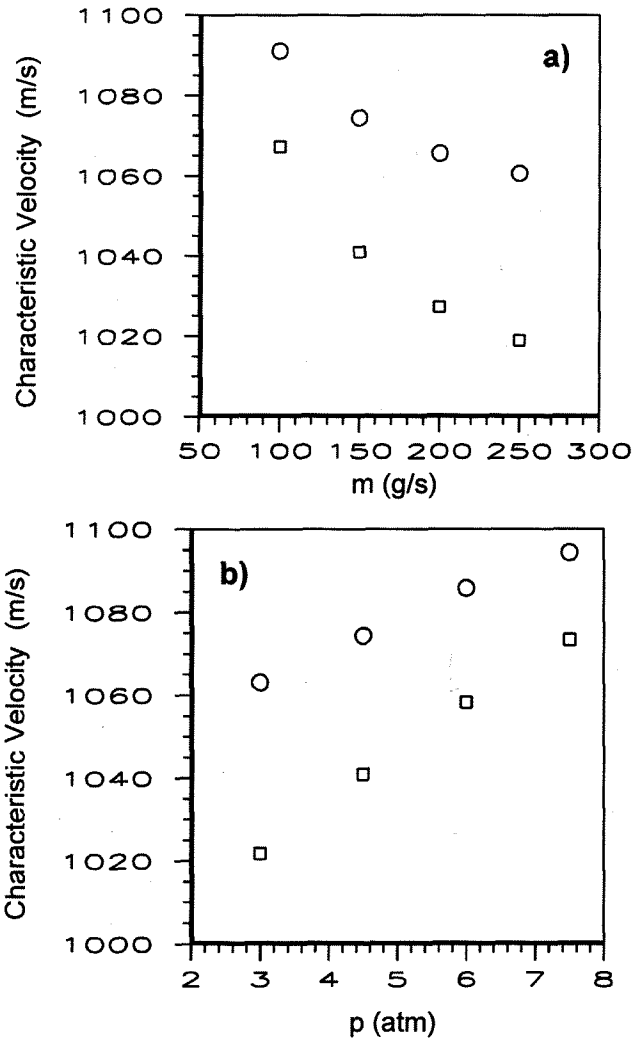

Figure 7 - Predicted characteristic velocity as a function of the air mass flow rate and pressure (o: using the average exit temperature; □ : using a temperature based on chemical equilibrium).

ACKNOWLEDGMENTS

This work has been supported by TNO, Prins Maurits Laboratory, in The Netherlands, within the framework of the workprogramme "Improvements and Updates of the COPPEF Code", and by the Portuguese Ministry of Defense.

REFERENCES

1. Schulte, G., "Fuel Regression and Flame Stabilization Studies", *J. Propulsion and Power*, Vol. 2, No. 4, 1986, pp. 301-304.

2. Schulte, G., Pein, R. and Högl, A., "Temperature and Concentration Measurements in a Solid Fuel Ramjet Combustion Chamber", *J. Propulsion and Power*, Vol. 3, No. 2, 1987, pp. 114-120.

3. Zvuloni, R., Gany, A. and Levy, Y., "Geometric Effects on the Combustion in Solid Fuel Ramjets", *J. Propulsion and Power*, Vol. 2, No. 4, 1986, pp. 301-304.

4. Zvuloni, R. , Levy, Y. and Gany, A., "Investigation of a Small Solid Fuel Ramjet Combustor", *J. Propulsion and Power*, Vol. 5, No. 3, 1989, pp. 269-275.

5. Ben-Arosh, R. and Gany, A., "Similarity and Scale Effects in Solid-Fuel Ramjet Combustors", *J. Propulsion and Power*, Vol. 8, No. 3, 1992, pp. 615-623.

6. Stevenson, C.A. and Netzer, D.W., "Primitive-Variable Model Applications to Solid-Fuel Ramjet Combustion", *J. Spacecraft and Rockets*, Vol. 18, No. 1, 1981, pp. 89-94.

7. Milshtein, T. and Netzer, D.W., "Three-Dimensional, Primitive-Variable Model for Solid-Fuel Ramjet Combustion", *J. Spacecraft and Rockets*, Vol. 23, No. 1, 1986, pp. 113-117.

8. Vos, J.B., "The Calculation of Turbulent Reacting Flows with a Combustion Model Based on Finite Chemical Kinetics", *Ph.D. thesis*, Delft University of Technology, Delft, The Netherlands, 1987.

9. Vos, J.B., "Calculating Turbulent Reacting Rlows Using Finite Chemical Kinetics", *AIAA J.*, Vol. 25, 1987, pp. 1365-1372.

10. van der Geld, C.W.M., Korting, P.A.O.G. and Wijchers, T., "Combustion of PMMA, PE and PS in a Ramjet", *Combustion and Flame*, Vol. 79, 1990, pp. 299-306.

11. Korting, P.A.O.G., van der Geld, C.W.M., Wijchers, T. and Schöyer, H.F.R., "Combustion of Polymethylmethacrylate in a Solid Fuel Ramjet", *J. Propulsion and Power*, Vol. 6, 1990, pp. 263-272.

12. Elands, P.J.M., Korting, P.A.O.G., Veraar, R.G. and Dijkstra, F., "Theoretical and Experimental Performance of a Solid Fuel Ramjet Combustor Cycle for Hypersonic Flight Conditions", *AGARD CP-479*, paper No. 29, 1990.

13. Elands, P., Korting, P. , Wijchers, T. and Dijkstra, F., "Comparison of Combustion Experiments and Theory in Polyethylene Solid Fuel Ramjets", *J. Propulsion and Power*, Vol. 6, 1990, pp. 732-739.

14. Coelho, P. J., Lemos, C., Carvalho, M.G. and Duic, N., "Modeling of a Solid Fuel Combustion Chamber of a Ramjet using a Multi-block Domain Decomposition Technique", AIAA paper No. 96-0847, 1996.

15. Chieng, C.C. and Launder, B.E., "On the Calculation of Turbulent Heat Transport Downstream from an Abrupt Pipe Expansion", *Numerical Heat Transfer*, Vol. 3, 1980, pp. 189-207.

16. Patankar, S.V. and Spalding, D.B., *Heat and Mass Transfer in Boundary Layers*, 2nd ed., Intertext Books, London, 1970.

17. Nallasamy, M., "Turbulence Models and Their Applications to the Predictions of Internal Flows: a Review", *Computers and Fluids*, Vol. 15, No. 2, 1987, pp. 151-194.

18. Cornelisse, J.W, Schöyer, H.F.R. and Wakker, K.F., *Rocket Propulsion and Space Flight Dynamics*, Pitman, London, 1979

19. Gordon, S. and McBride, B.J., "Computer Program for Calculation of Complex Chemical Equilibrium Compositions, Rocket Performance, Incident and Reflected Shocks, and Chapman-Jouguet Detonations", NASA SP-273, NASA, Washington, 1971.